

# Exploring the Anticancer Potential of *C. Cartilaginea* Fruit Extract: Gene Expression and Pathway Analysis in Prostate Cancer Cells

Maram Bakr Hosawi<sup>1</sup>, Hala Salim Sonbol <sup>2\*</sup>, Salman Bakr Hosawi<sup>1</sup>

<sup>1</sup>Department of Biochemistry, Faculty of Science, King Abdulaziz University, Jeddah, Kingdom of Saudi Arabia.

<sup>2</sup>Correspondence: Hala Salim Sonbol, Department of Biochemistry, Faculty of Science, King Abdulaziz University, Jeddah, Kingdom of Saudi Arabia. [hsonbol@kau.edu.sa](mailto:hsonbol@kau.edu.sa)

Prostate cancer (PCa) is a leading cause of male cancer-related deaths in developed countries, surpassed only by lung and colorectal cancer. Although advancements have been made in surgical, radiation, hormonal, and medical therapies, the treatment of advanced-stage PCa still poses challenges. Consequently, exploring alternative approaches, such as dietary cancer chemopreventive agents, to reduce PCa incidence is of great interest. Plant-derived products have been proposed as potential therapies for cancer treatment. In this study, we systematically analyzed molecular correlates of the effect of *C. cartilaginea* fruit extract on the PCa cell line by bioinformatics analysis. Differentially expressed genes (DEGs) and differentially methylated genes (DMGs) were filtered out from the GSE69223 and GSE84749 dataset and subjected to the gene ontology (GO) and Kyoto Encyclopedia of Genes and Genomes (KEGG) pathway analyses. The protein-protein interactions (PPI) network was constructed, followed by the identification of hub genes. A total of 69 DEGs and DMGs were identified. Among these DEGs and DMGs genes, seven hub genes were significantly enriched in regulating cell population and proliferation. (ARX, NKX2-3, SCGB3A1, CCND2, TRPM4, NRG1, SFRP2 ) and twenty hub genes were significantly enriched in the organization of extracellular matrix and cell-matrix, cell growth and division, cell adhesion, cell migration, cell cycle, cell motility, and apoptotic process (FBLN5, COL9A2, COL6A1, MMP14, MMP16, THBS4, SPON1, EDIL3, CCND2, NRG1, DAB1, SCGB3A1, SFRP2, GPC6, NAV3, HIF3A, PLSCR1, ACTC1, PHACTR1, OCA2 ). To relate this finding with our previous study we supposed that the extract might affect genes that take part in the regulation of cell proliferation, division, growth, cell cycle, and apoptotic process this is likely to have a role in cell death in MTT assay. However, in the scratch assay outcome, the width of the scratch area widely opened and cells appear to die rather than moving across the scratch, we assumed that this could be due to the effect of the extract on genes that participate in the organization of cell-matrix, extracellular matrix. Also participate in regulating cell adhesion, migration, and motility. In future studies, we suggest the use of other parts of the *C. cartilaginea* plant such as the stem, roots, and leaves on human normal prostate and PCa cells. Also, study the effect of the *C. cartilaginea* fruit extract on SCGB3A1 and THBS4 expression.

## Introduction

Prostate cancer (PCa) ranks as the second most prevalent disease globally, according to the World Health Organization, with 1,414,259 new cases reported worldwide. This places it as the fifth leading cause of cancer-related deaths in men. Global Cancer Statistics for 2020 estimated that PCa resulted in 375,304 deaths among men of all ages. In countries like the United States, Africa, and Europe, PCa is the second leading cause of death following lung cancer (GLOBOCAN 2020). In Saudi Arabia, the International Agency for Research on Cancer projected 693 cases of PCa in 2020, with an age-standardized incidence rate of 7 per 100,000 men and an age-standardized mortality rate of 2.5 per 100,000 men (Panigrahi et al. 2019). Arab countries exhibit relatively lower age-standardized rates of PCa compared to Europe and North America, which could be attributed to factors such as limited prostate-specific antigen screening and unique biological distinctions among Arab men (Osman et al. 2018; Belkahla et al. 2022).

Hence, Comprehending the underlying molecular mechanisms implicated in the onset and advancement of PCa holds significant clinical implications (Vogelstein et al. 2013). Consequently, there is an urgent imperative to uncover dependable and efficient biomarkers and ascertain the involvement of genes in PCa's biological processes. Microarray and bioinformatics techniques, along with the Gene Expression Online Database (GEO), are extensively employed for screening differentially expressed genes (DEGs), investigating molecular signals and their interrelationships, facilitating the construction of gene regulatory networks, and analyzing differential expression patterns between cancerous and healthy cells. This endeavor aims to identify novel diagnostic and therapeutic biomarkers (Clough and Barrett 2016).

The current study evaluated the potential molecular mechanisms and biomarkers of PCa using a bioinformatics approach. Microarray expression data were downloaded from the Gene Expression Omnibus (GEO) database. The DEGs and DMGs were subjected to functional and pathway enrichment analysis, followed by protein-protein interaction (PPI) network.

## **Material and methods**

### **Microarray Data**

Two gene expression profile was downloaded from public domains (NCBI-Gene Expression Omnibus (GEO) repository). GSE69223: Genome-wide analysis of gene expression patterns in human PCa and GSE84749: Genome-wide DNA methylation profiling of prostate specimens from a clinical trial of genistein supplementation before prostatectomy (Bilir et al. 2017; Meller et al. 2016).

The original dataset in the GSE69223 study includes fifteen non-cancerous and fifteen primary prostate tumors samples. The researcher investigated the mechanisms of PCa progression, by performing mRNA expression profiling of human PCa and benign tissues (Meller et al. 2016), while in GSE84749 study, the genome-wide DNA methylation profiles were performed on a total of 24 prostate samples from tumor or normal tissues. The previous

study was carried out to identify the molecular effects of genistein on DNA methylation in prostate cancer, the authors compared DNA methylation profiles of genistein-treated tumors with placebo-treated samples. There were 156 probes with significantly increased methylation in placebo-treated cases versus normal tissues that were not significant between genistein-treated cases and normal tissues, suggesting that genistein may have had some demethylation effects (Bilir et al. 2017). The results and values from both datasets were handled and normalized using R software (Limma and GEOquary packages).

### **Data Processing And Screening of Differentially Expressed and Methylated Genes**

To ensure the quality and comparability of the samples of the different datasets, we inspected the median of the normalized sample values. Then we identify genes that are significantly expressed or methylated either positively or negatively in both studies, we plotted the fold change (logFC) versus the adjusted P-value (Adj.P-Val) in a volcano plot, and the cut-off values were set to highlight genes with significant changes. We used various computer software programs to analyze differentially expressed genes (DEGs) and differentially methylated genes (DMGs).

Then, to find common genes between expression and methylation studies we used the gene symbol from each dataset and represented the common genes using Venn's diagrams (Venny 2.1). This resulted in four sub-categories: First, overexpressed and hypermethylated, we compared upregulated genes in expression study with the hypermethylated genes in methylation. Second, overexpressed and hypomethylated. Third, under-expressed and hypermethylated. Finally, under-expressed and hypomethylated. At that point, gene names were obtained from the gene symbol using BIOGPS.ORG (Wu et al. 2016).

### **Integration of the Protein-Protein Interaction Network**

Protein-protein interaction analysis serves as an entry point for better interpretation of relationships between different proteins on a genome-wide scale, and might be helpful to provide novel insights into protein function explanation (Stelzl et al. 2005). We investigate the integration of the PPI network between the DEGs and DMGs in the sub-categories, we used the Search Tool for the Retrieval of Interacting Genes STRING version 11. (<http://string-db.org/>) (Von Mering et al. 2003) for the exploration of potential DEGs and DMGs interactions at the protein level (Szklarczyk et al. 2015; Franceschini et al. 2013). The direct interactions between the acquired genes were perceived by changing the confidence from medium confidence (0.400) to low confidence (0.150) to increase the chance of evidence. Whilst, indirect interactions between genes were detected by adding a second shell (no more than 20 interactor) and restoring confidence to medium confidence (0.400).

### **Gene Ontology and Pathway Enrichment Analysis of DEGs and DMGs**

The identified DEGs and DMGs were uploaded to the online software Enricher (Kuleshov et al. 2016; Chen et al. 2013) for Gene Ontology (GO) enrichment and Kyoto Encyclopedia of Genes and Genomes (KEGG) pathway analyses a database regarding genomes, biological pathways, diseases, drugs and chemical substances (Kanehisa and Goto 2000). To characterize the function and pathway of DEGs and DMGs, Gene Ontology was used to define gene functions in three aspects: molecular function (MF), cellular component (CC), and biological

process (BP). Gene Ontology was applied to identify BP of DEGs and DMGs. The PPI was also identified. Then, pathway analysis and functional annotation for DEGs and DMGs were performed using UniProt (The UniProt Consortium 2019).  $P < 0.05$  was considered to indicate a statistically significant difference.

## Results

### Bioinformatic Analysis of PCa Transcriptomics and Methylation Datasets

#### Identification of DEGs and DMGs

In a volcano plot result, 264 were upregulated by more than 1.5-fold, while 605 genes were downregulated by at least  $-1.5$ -fold (Figure 1). The methylation data exhibited 3661 hypermethylated genes by more than 0.2-fold, and 370 hypomethylated genes by at least  $-0.2$ -fold (Figure 2).

The common genes found between expression and methylation studies represented using Venn diagrams resulted in four sub-categories: First, upregulated and hypermethylated, seven common genes were found among thousands of genes. Second, upregulated and hypomethylated, nine common genes were found. Third, downregulated and hypermethylated, fifty common genes were found. Finally, downregulated and hypomethylated, four common genes were found (Figures 3 - 6). The gene names obtained from the gene symbol using BIOGPS.ORG (Tables 1 - 6).

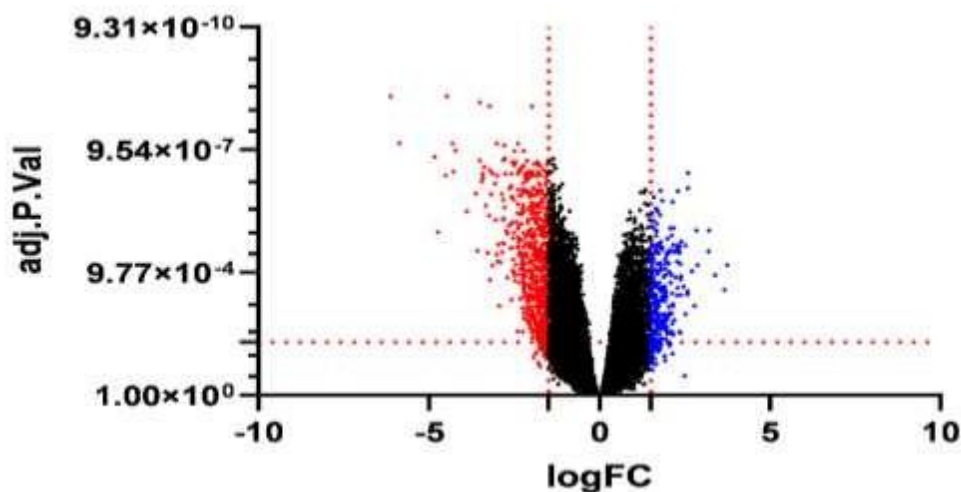


**Figure 1.** Volcano Plot of GSE69223 Expression Dataset, logFC versus adj.P.Val, Blue Dots Represents Positively Expressed Gene ( $\geq 1.5$ ), Red Dots Represents Negatively Expressed Gene ( $\leq -1.5$ ), Black Dots Represents Non-significant Genes.

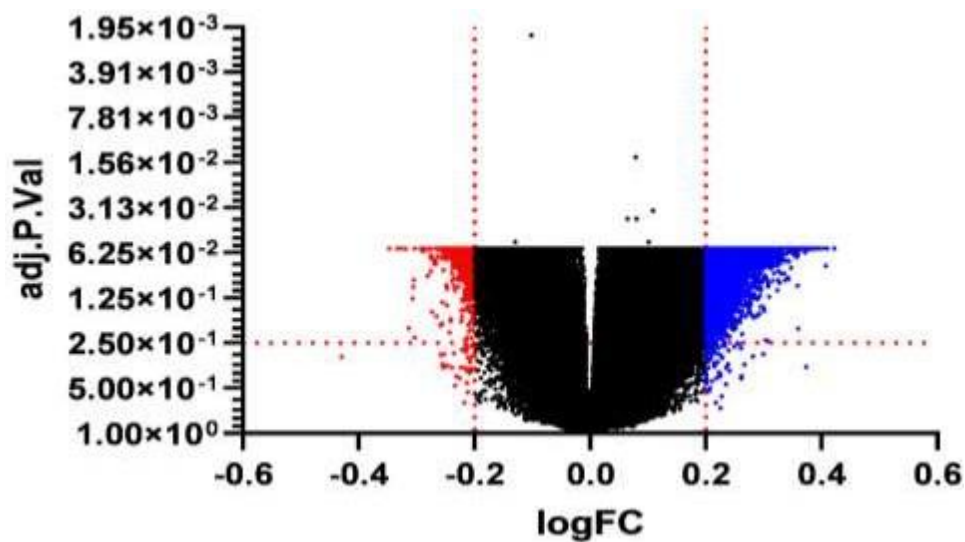


**Figure 2.** Volcano Plot of GSE84749 Methylation Dataset, logFC versus adj.P.Val, Blue Dots Represents Positively Methylated Gene ( $\geq 0.2$ ), Red Dots Represents Negatively Methylated Gene ( $\geq -0.2$ ), Black Dots Represents Non-significant Genes.

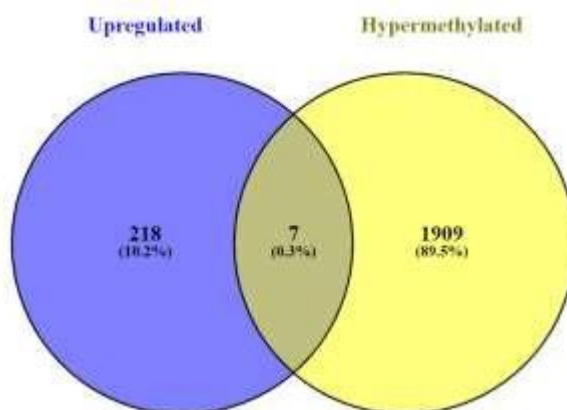


**Figure 3.** Venn Diagram Analysis of DEGs and DMGs. Blue Circle Represents the Upregulated Genes, Yellow Circle Represents Hypermethylated Genes. The Intersection of the Two Circles Represents Overlapping of DEGs and DMGs Among the Two Datasets. DEGs, differentially expressed genes. DMGs, differentially methylated genes.

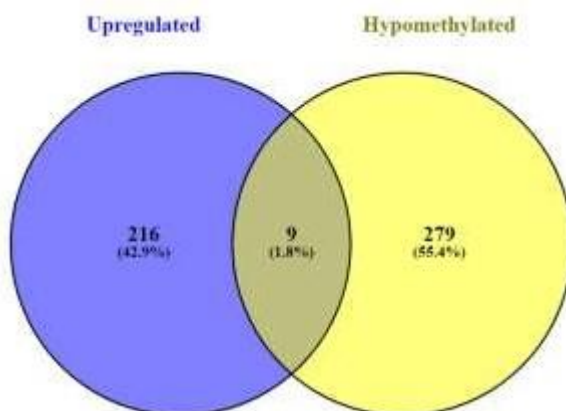


**Figure 4.** Venn Diagram Analysis of DEGs and DMGs. Blue Circle Represents the Upregulated Genes, Yellow Circle Represents Hypomethylated Genes. The Intersection of the Two Circles Represents Overlapping of DEGs and DMGs Among the Two Datasets. DEGs, differentially expressed genes. DMGs, differentially methylated genes.

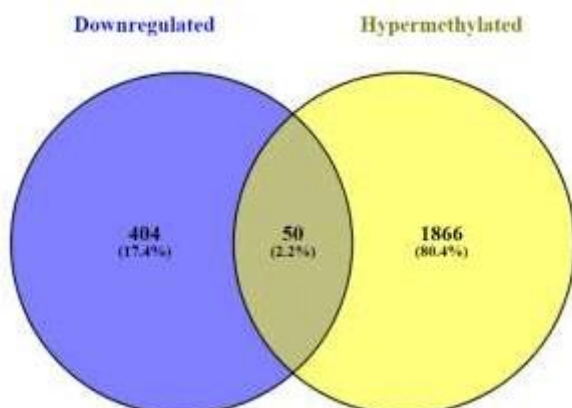


**Figure 5.** Venn Diagram Analysis of DEGs and DMGs. Blue Circle Represents the Downregulated Genes, Yellow Circle Represents Hypermethylated Genes. The Intersection of the Two Circles Represents Overlapping of DEGs and DMGs Among the Two Datasets. DEGs, differentially expressed genes. DMGs, differentially methylated genes

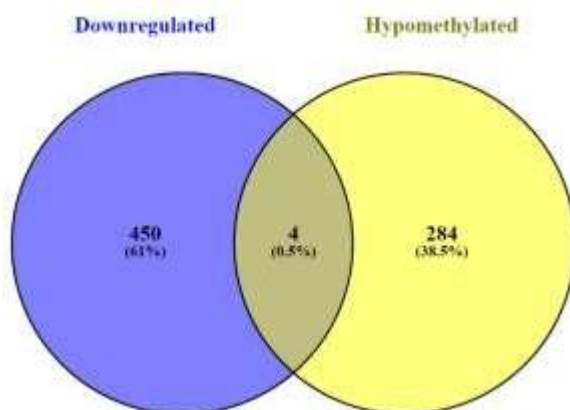


**Figure 6.** Venn Diagram Analysis of DEGs and DMGs. Blue Circle Represents the Downregulated Genes, Yellow Circle Represents Hypomethylated Genes. The Intersection of the Two Circles Represents Overlapping of DEGs and DMGs Among the Two Datasets. DEGs, differentially expressed genes. DMGs, differentially methylated genes



**Table 1.** Names of genes obtained from the gene symbol (upregulated and hypermethylated).  
Data are expressed as fold change (logFC) versus the adjusted P-value (Adj.P-Val).

Gene Name	Gene Symbol	Expression		Methylation	
		logFC	Adj.P-Val	logFC	Adj.P-Val
<b>Thrombospondin 4</b>	<b>THBS4</b>	2.0749	0.00008	0.223	0.07948
FEV Transcription Factor, ETS Family Member	FEV	2.198687	0.000309	0.217	0.05822
<b>Collagen Type IX Alpha 2 Chain</b>	<b>COL9A2</b>	1.693973	0.00105	0.227	0.05822
Protein Phosphatase, Mg2+/Mn2+ Dependent 1H	PPM1H	1.23484	0.00125	0.0703	0.07828
<b>NK2 Homeobox 3</b>	<b>NKX2-3</b>	2.01996	0.0534	0.163	0.11502
Arachidonate 15-Lipoxygenase	ALOX15	1.531027	0.091	0.216	0.05822
Aristaless Related Homeobox	ARX	1.51848	0.12	0.208	0.05822

**Table 2.** Names of genes obtained from the gene symbol (upregulated and hypomethylated).  
Data are expressed as fold change (logFC) versus the adjusted P-value (Adj.P-Val).

Gene Name	Gene Symbol	Expression		Methylation	
		logFC	Adj.P-Val	logFC	Adj.P-Val
<b>Transient Receptor Potential Cation Channel Subfamily M Member 4</b>	<b>TRPM4</b>	2.597787	0.00000347	-0.268	0.06987
Elongation Factor for RNA Polymerase II 3	ELL3	1.646287	0.0000259	-0.2	0.07695
Fatty Acid Synthase	FASN	1.676227	0.0000616	-0.167	0.06172
Thrombospondin 4	THBS4	2.0749	0.00008	-0.241	0.05844
Claudin 8	CLDN8	2.16216	0.000203	-0.224	0.0828
Growth Differentiation Factor 15	GDF15	2.331587	0.000322	-0.275	0.05876
Coiled-Coil Domain Containing 154	CCDC154	1.505267	0.0643	-0.21	0.05822
Tudor Domain Containing 1	TDRD1	1.904193	0.107	-0.191	0.06082
<b>Aristaless Related Homeobox</b>	<b>ARX</b>	1.51848	0.12	-0.21	0.05822



**Table 3.** Names of genes obtained from the gene symbol (downregulated and hypermethylated).

Gene Name	Gene Symbol	Expression		Methylation	
		logFC	Adj.P-Val	logFC	Adj.P-Val
Potassium Inwardly Rectifying Channel Subfamily J Member 3	KCNJ3	-4.48877	0.0000000457	0.238	0.05844
Forkhead Box F2	FOXF2	-3.01717	0.000000667	0.22	0.14876
GATA Binding Protein 6	GATA6	-2.49865	0.00000101	0.313	0.05822
<b>Spondin 1</b>	<b>SPON1</b>	-2.2063	0.00000368	0.205	0.094
Coiled-Coil Domain Containing 8	CCDC8	-2.06934	0.00000461	0.228	0.05844
Carbonic Anhydrase 3	CA3	-3.06466	0.00000639	0.216	0.07375
Nik Related Kinase	NRK	-2.39763	0.0000208	0.15	0.09383
Keratin 222	KRT222	-2.106246	0.0000483	0.162	0.15439
Potassium Voltage-Gated Channel Subfamily E Regulatory Subunit 3	KCNE3	-2.18787	0.000181	0.0337	0.08476
Eukaryotic Translation Initiation Factor 4E Binding Protein 2	EIF4EBP2	-2.34837	0.000347	0.237	0.05844
PNMA Family Member 8B	PNMAL2	-2.23308	0.000389	0.281	0.06303
Phosphodiesterase 1C	PDE1C	-1.85089	0.000795	0.175	0.11315
UBX Domain Protein 10	UBXN10	-2.23487	0.0013	0.224	0.08224
V-Set and Transmembrane Domain Containing 2A	VSTM2A	-2.93774	0.00641	0.279	0.05916
<b>DAB Adaptor Protein 1</b>	<b>DAB1</b>	-2.09591	0.00661	0.26	0.05844
<b>Secretoglobin Family 3A Member 1</b>	<b>SCGB3A1</b>	-2.21419	0.00939	0.343	0.05822

Fibroblast Growth Factor 14	FGF14	-2.22799	0.0126	0.153	0.10438
-----------------------------	-------	----------	--------	-------	---------

**Cont. Table 4.** Names of genes obtained from the gene symbol (downregulated and hypermethylated).

Gene Name	Gene Symbol	Expression		Methylation	
		logFC	Adj.P-Val	logF C	Adj.P-Val
JAZF Zinc Finger 1	JAZF1	-1.73276	0.00000392	0.228	0.05844
Microtubule Associated Protein 1B	MAP1B	-2.14266	0.00000445	0.209	0.14234
<b>Cyclin D2</b>	<b>CCND2</b>	-1.69957	0.000101	0.224	0.05822
<b>Collagen Type VI Alpha 1 Chain</b>	<b>COL6A1</b>	-1.63162	0.00012	0.257	0.07047
<b>EGF Like Repeats and Discoidin Domains 3</b>	<b>EDIL3</b>	-1.86623	0.000255	0.205	0.06366
<b>Secreted Frizzled Related Protein 2</b>	<b>SFRP2</b>	-1.69924	0.000311	0.201	0.09821
<b>Hypoxia Inducible Factor 3 Subunit Alpha</b>	<b>HIF3A</b>	-1.89208	0.000652	0.389	0.05822
<b>OCA2 Melanosomal Transmembrane Protein</b>	<b>OCA2</b>	-1.65663	0.00247	0.225	0.12509
MCF.2 Cell Line Derived Transforming Sequence	MCF2	-1.91317	0.0025	0.254	0.05962
Tensin 1	TNS1	-1.86568	0.00371	0.203	0.06225
Ring Finger Protein 165	RNF165	-1.62829	0.00545	0.222	0.0632
GIPC PDZ Domain Containing Family Member 2	GIPC2	-1.71199	0.00667	0.207	0.10985
<b>Neuron Navigator 3</b>	<b>NAV3</b>	-1.66649	0.0179	0.204	0.05822
<b>Phospholipid Scramblase 1</b>	<b>PLSCR1</b>	-1.68093	0.019	0.204	0.17237
<b>Neuregulin 1</b>	<b>NRG1</b>	-1.76891	0.0231	0.203	0.0859
N-Acetylated Alpha-Linked Acidic Dipeptidase 2	NAALA D2	-1.64403	0.105	0.201	0.09672

Data are expressed as fold change (logFC) versus the adjusted P-value (Adj.P-Val).

Gene Name	Gene Symbol	Expression		Methylation	
		logFC	Adj.P-Val	logF C	Adj.P-Val
Nudix Hydrolase 10	NUDT10	- 1.5052 9	0.0000054 2	0.219	0.09873
<b>Glypican 6</b>	<b>GPC6</b>	- 1.5795 7	0.0000347	0.238	0.05822
<b>Fibulin 5</b>	<b>FBLN5</b>	- 1.5613 9	0.0000483	0.269	0.05844
Retinoic Acid Receptor Responder 2	RARRES 2	- 1.5335 7	0.0000558	0.202	0.059
S100 Calcium Binding Protein A6	S100A6	- 1.5394 6	0.000421	0.25	0.06146
PPARG Coactivator 1 Alpha	PPARGC 1A	- 1.5919 6	0.00212	0.208	0.16401
Pleckstrin Homology, Myth4 And FERM Domain Containing H2	PLEKHH 2	- 1.5406 9	0.00626	0.277	0.05822
<b>Matrix Metalloproteinase 14</b>	<b>MMP14</b>	- 1.5620 5	0.00735	0.212	0.06622
<b>Actin Alpha Cardiac Muscle 1</b>	<b>ACTC1</b>	- 1.6159 9	0.0103	0.267	0.06601
<b>Phosphatase and Actin Regulator 1</b>	<b>PHACT R1</b>	- 1.5722 9	0.016	0.267	0.08006
CAP-Gly Domain Containing Linker Protein Family Member 4	CLIP4	- 1.5406 3	0.0193	0.237	0.06784

Ras And Rab Interactor 3	RIN3	- 1.6262 3	0.0281	0.231	0.06985
Cerebellin 4 Precursor	CBLN4	- 1.5560 3	0.0316	0.291	0.05822
Trimethyllysine Hydroxylase, Epsilon	TMLHE	- 1.5456 3	0.0392	0.209	0.05822
Butyrophilin Like 9	BTNL9	- 0.9058 5	0.056	0.209	0.29829
Myelin Transcription Factor 1 Like	MYT1L	- 1.6009 8	0.066	0.204	0.0622

**Cont. Table 5.** Names of genes obtained from the gene symbol (downregulated and hypermethylated).

Data are expressed as fold change (logFC) versus the adjusted P-value (Adj.P-Val).

**Table 6.** Names of genes obtained from the gene symbol (downregulated and hypomethylated).

Data are expressed as fold change (logFC) versus the adjusted P-value (Adj.P-Val).

Gene Name	Gene Symbol	Expression		Methylation	
		logFC	Adj.P-Val	logFC	Adj.P-Val
Thyrotropin Releasing Hormone Degrading Enzyme	TRHDE	- 2.55095	0.0000019	-0.202	0.06338
<b>Matrix Metalloproteinase 16</b>	<b>MMP16</b>	- 1.77959	0.0000237	-0.216	0.09648
Transmembrane Protein 132C	TMEM132C	- 2.55686	0.000237	-0.2	0.05822
FAT Atypical Cadherin 3	FAT3	- 1.60044	0.00558	-0.202	0.05822

### **PPI Network**

Protein-protein interactions network between DEGs and DMGs in the sub-categories were perceived. Among upregulated and hypermethylated genes direct interactions between COL9A2 and THBS4 were found. Whereas, COL9A2 and THBS4 indirectly interact with ALOX15 (Figures 7 A and B). In upregulated and hypomethylated genes, FASN was found to interact directly with GDF15 and indirectly with TDRD1 (Figures 8 A and B). Amongst downregulated and hypermethylated genes, almost all genes are directly interacting with each other except NRK, UBXN10, JAZF1, OCA2, NAALAD2, RNF165, and BTNL9 genes. Also, it was found that these genes interact indirectly with each other but not as much as direct interactions (Figures 9 and 10). Lastly, among downregulated and hypomethylated genes, only MMP16 and FAT3 were found to interact directly and indirectly with each other (Figures 11 A and B).

### **Kyoto Encyclopedia of Genes and Genomes (KEGG) Pathway**

KEGG pathway analysis revealed that the upregulated DEGs were highly associated with pathways including ECM-receptor interaction, focal adhesion, PI3K-Akt pathway, ferroptosis, and fatty acid synthesis (Figures 12 and 13). While, the downregulated DEGs were enriched in the protein adhesion, longevity regulating pathways, and parathyroid hormone synthesis, secretion, and action (Figures 14 and 15).

According to the biological process's analysis, DEGs and DMGs were mainly associated with the regulation of cell growth, adhesion, migration, and motility. Along with the regulation of the extracellular matrix, the cell-matrix and several different pathways (Table 7). The PPI amid the DEGs and DMGs (Figure 16).

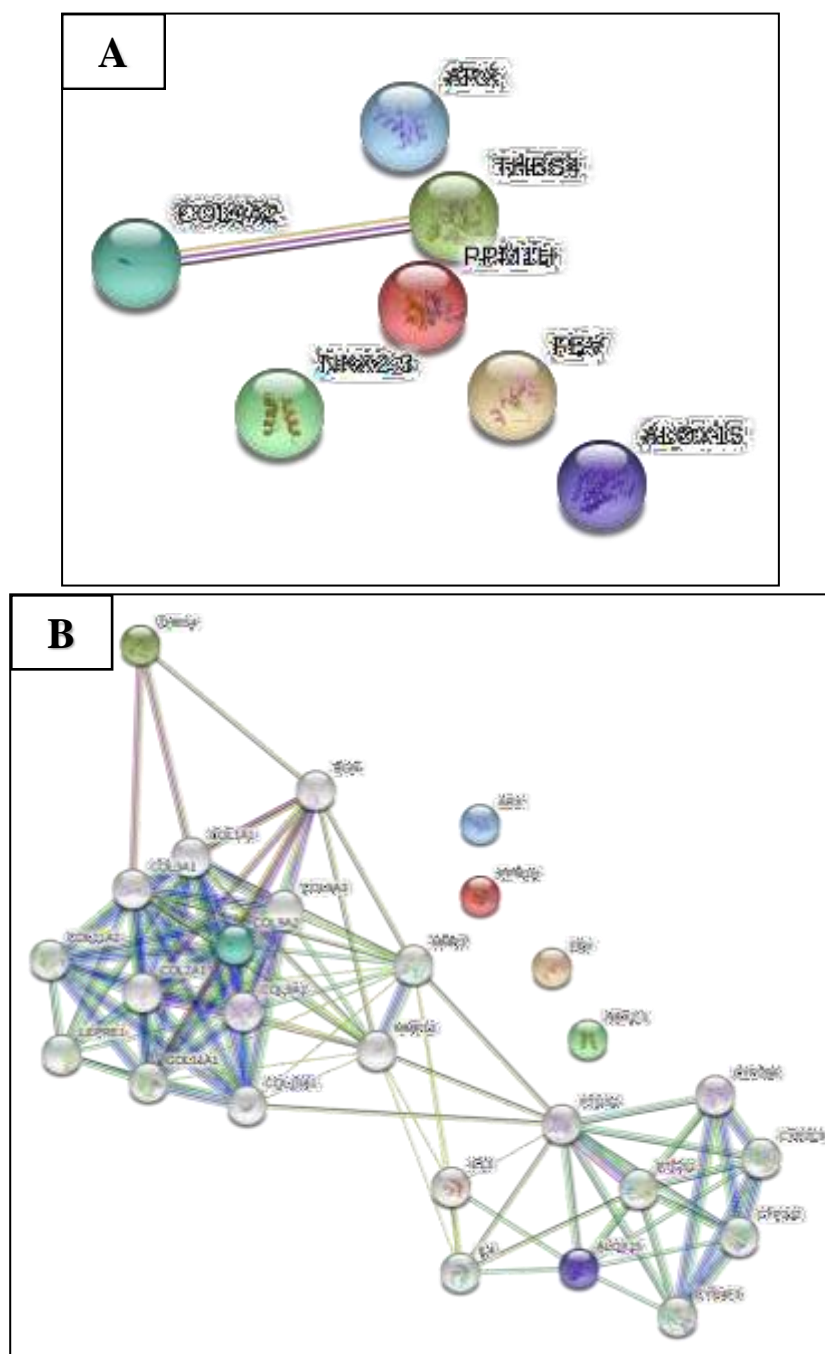


**Figure 7.** PPI Network of DEGs and DMGs. **A.** Direct Interactions. **B.** Indirect Interactions Among Upregulated and Hypermethylated Genes. Colored Nodes: Query Proteins and First Shell of Interactors. White Nodes: Second Shell of Interactors. Line Color Indicates the Type of Interaction Evidence: Experimentally Determined, Textmining, Co-expression, From Curated Databases, Co-occurrence, Protein Homology.

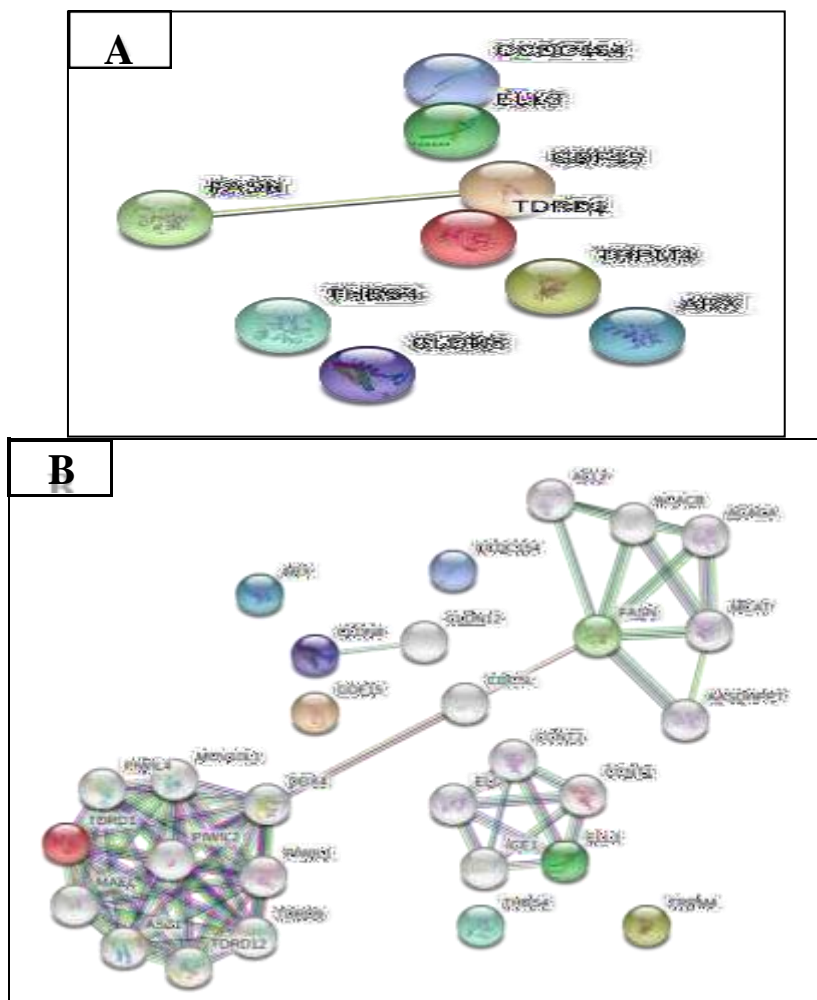




**Figure 8.** PPI Network of DEGs and DMGs. **A.** Direct Interactions. **B.** Indirect Interactions Among Upregulated and Hypomethylated Genes. Colored Nodes: Query Proteins and First Shell of Interactors. White Nodes: Second Shell of Interactors. Line Color Indicates the Type of Interaction Evidence: Experimentally Determined (red), Textmining (blue), Co-expression (green), From Curated Databases (yellow), Gene Neighborhood (purple), Protein Homology (orange), Gene Fusions (pink).

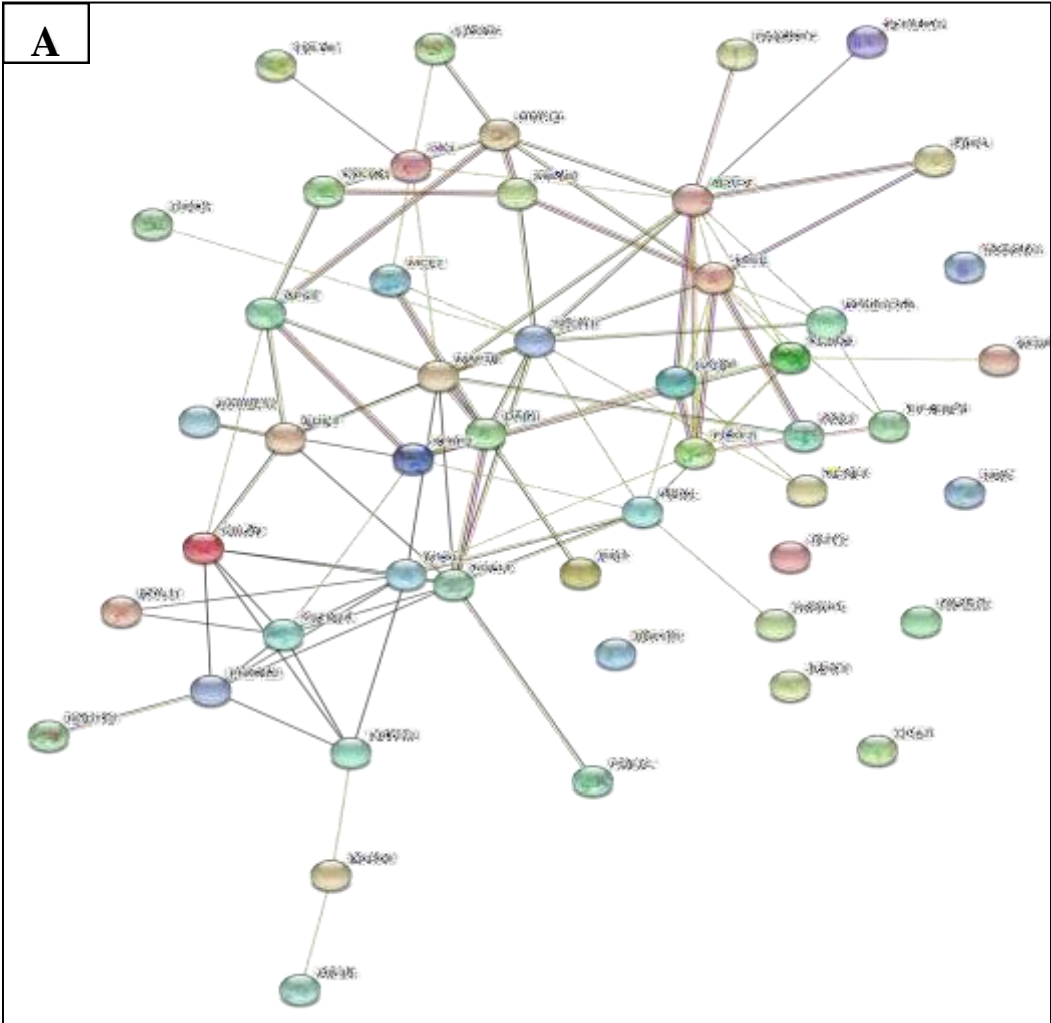


**Figure 9.** PPI Network of DEGs and DMGs. **A.** Direct Interactions Among Downregulated and Hypermethylated Genes. Colored Nodes: Query Proteins and First Shell of Interactors. White Nodes: Second Shell of Interactors. Line Color Indicates the Type of Interaction Evidence. ●● Experimentally Determined. ●● Textmining. ●● Co-expression. ●● From Curated Databases.

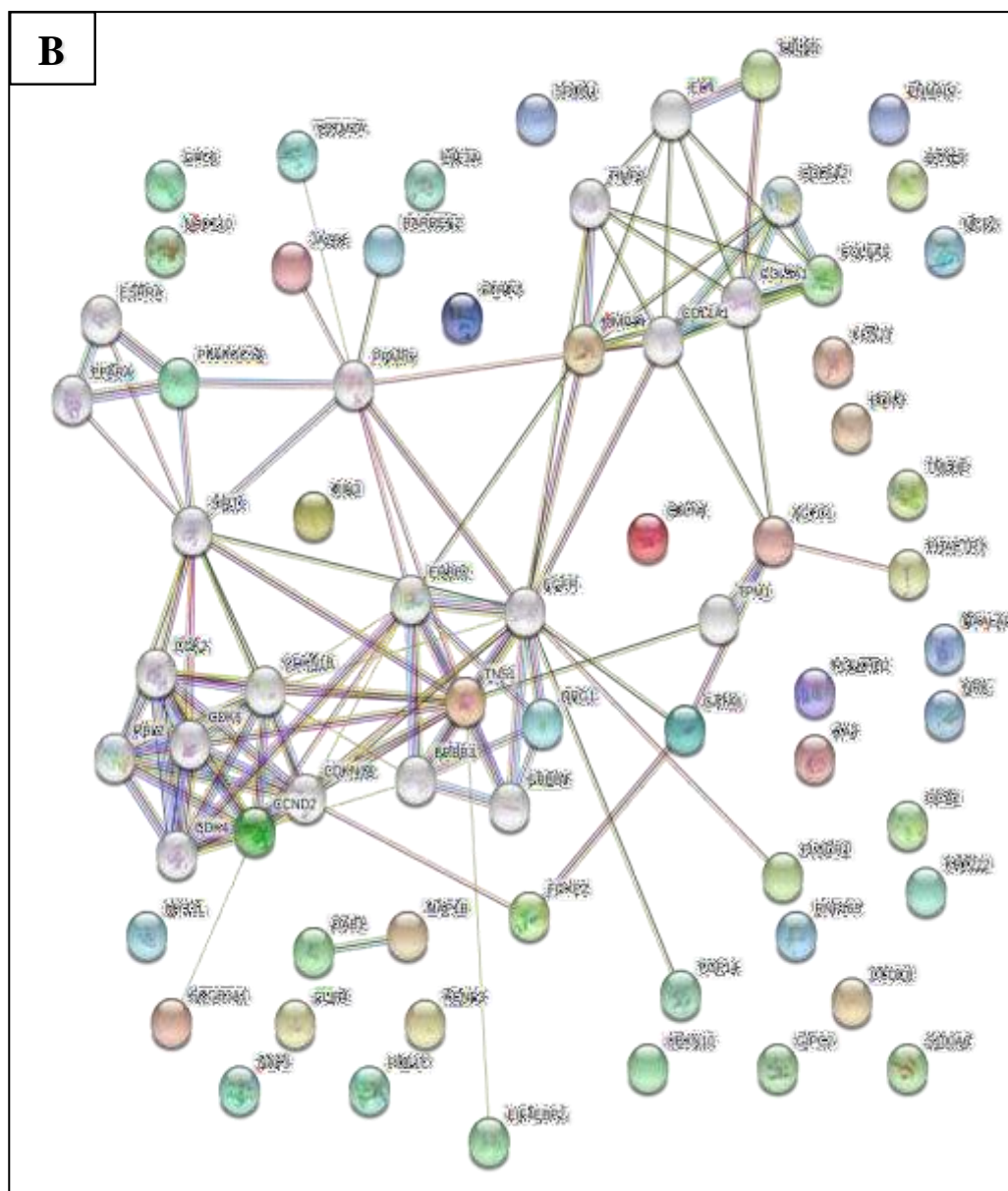


**Figure 10.** PPI Network of DEGs and DMGs. **B.** Indirect Interactions Among Downregulated and Hypermethylated Genes. Colored Nodes: Query Proteins and First Shell of Interactors. White Nodes: Second Shell of Interactors. Line Color Indicates the Type of Interaction Evidence. ●—● Experimentally Determined, ●—● Textmining, ●—● Co-expression, ●—● From Curated Databases, ●—● Protein Homology, ●—● Gene Co-occurrence

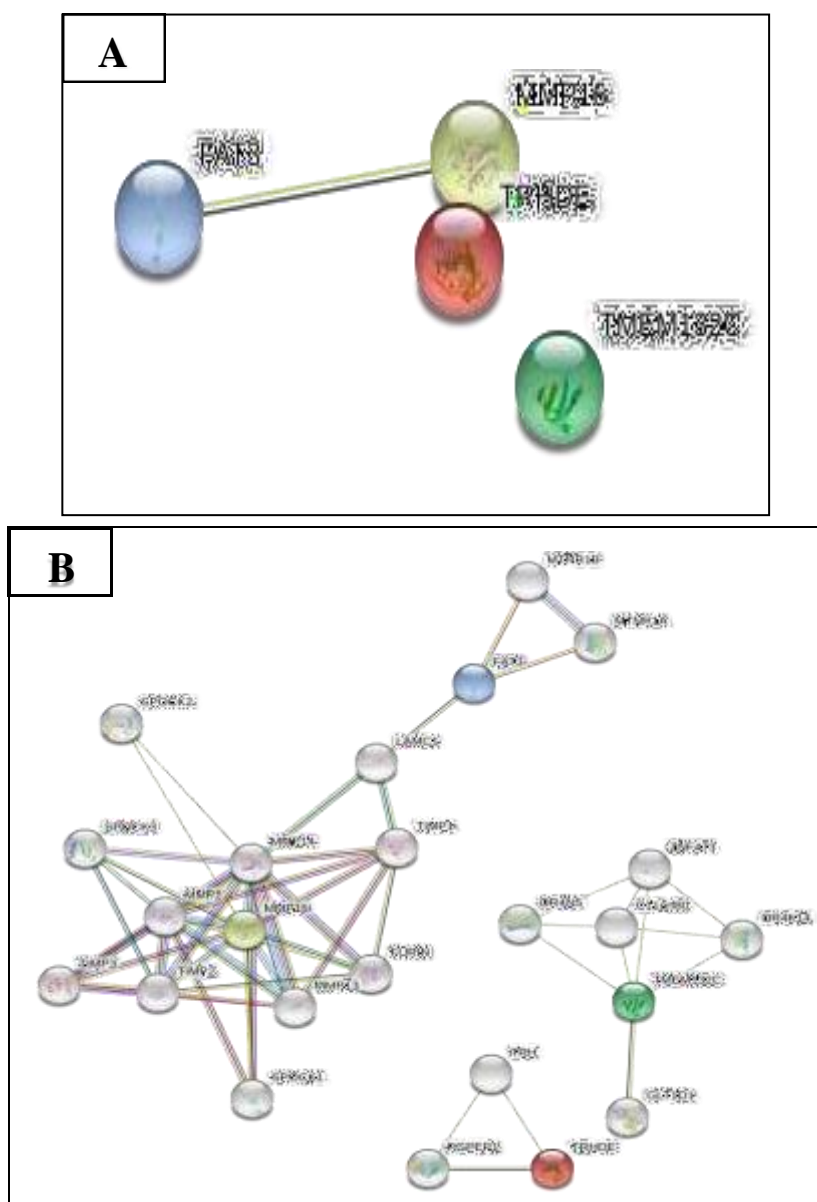


**Figure 11.** PPI Network of DEGs and DMGs. **A.** Direct Interactions. **B.** Indirect Interactions Among Downregulated and Hypomethylated Genes. Colored Nodes: Query Proteins and First Shell of Interactors. White Nodes: Second Shell of Interactors. Line Color Indicates the Type of Interaction Evidence. ●—● Experimentally Determined. ●—● Textmining. ●—● Co-expression. ●—● From Curated Databases. ●—● Protein Homology. ●—● Gene Co-occurrence. ●—● Gene Fusions

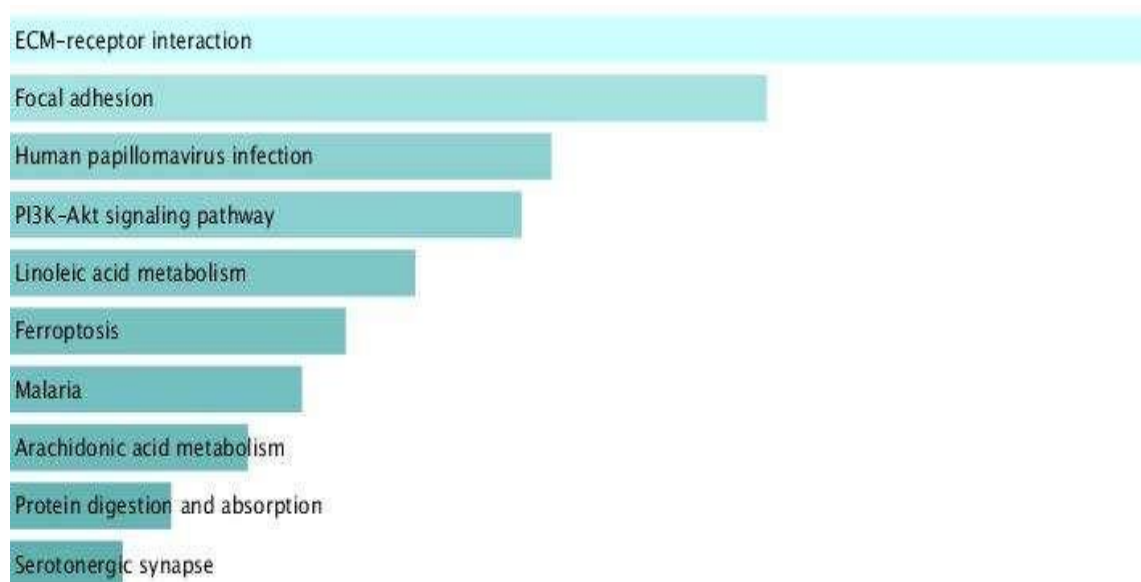


**Figure 12.** KEGG pathway analysis of DEGs and DMGs. DEGs of upregulated and hypermethylated overlapping. Bars sorted by P-value ranking. KEGG, kyotoencyclopedia of genes and genome.

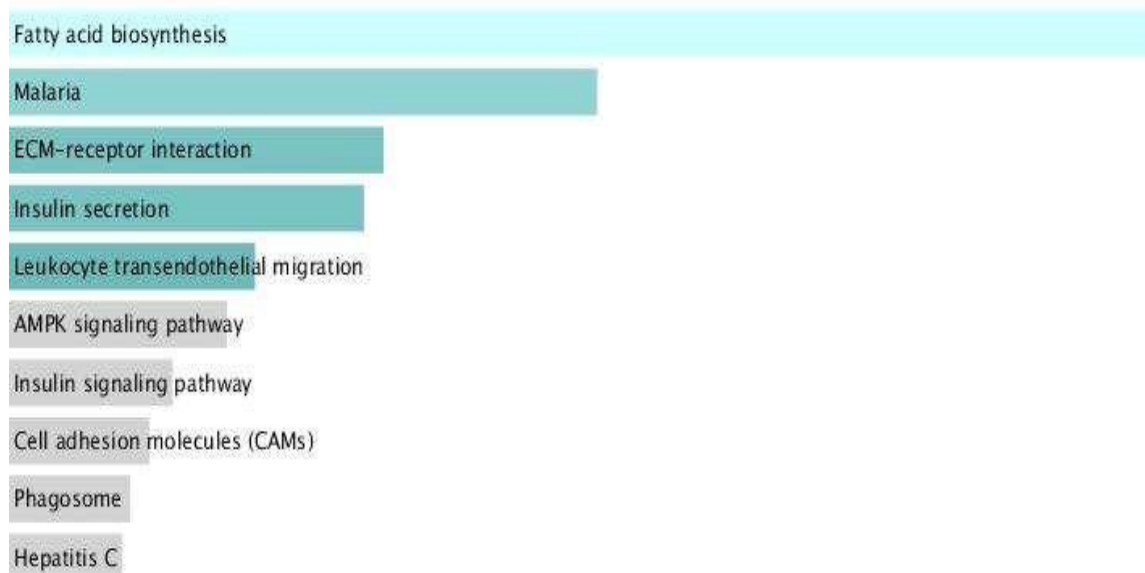


**Figure 13.** KEGG pathway analysis of DEGs. DEGs of upregulated and hypomethylated overlapping. Bars sorted by P-value ranking. KEGG, kyoto encyclopedia of genes and genome. DEGs, differentially expressed genes.

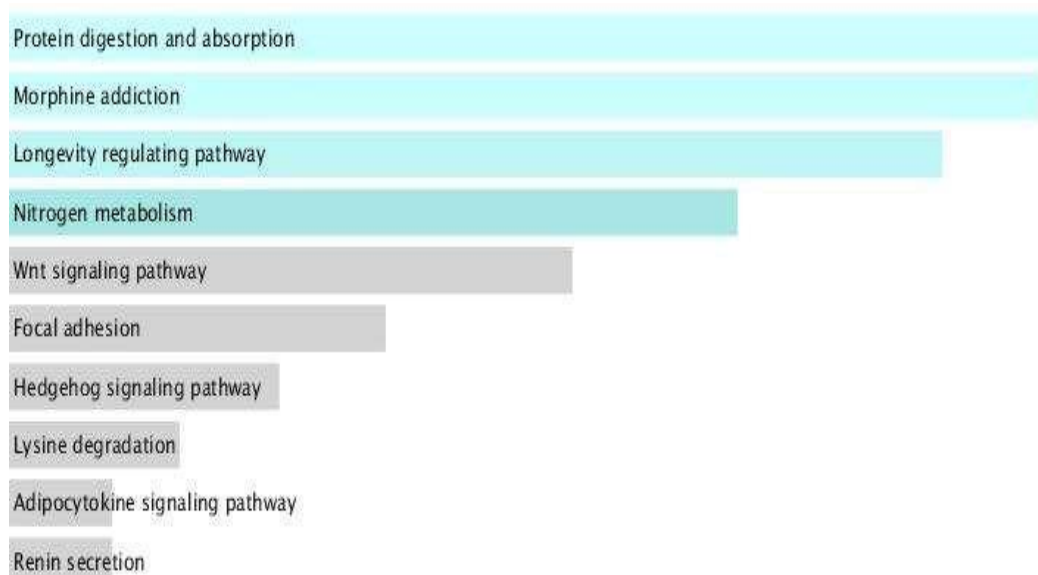


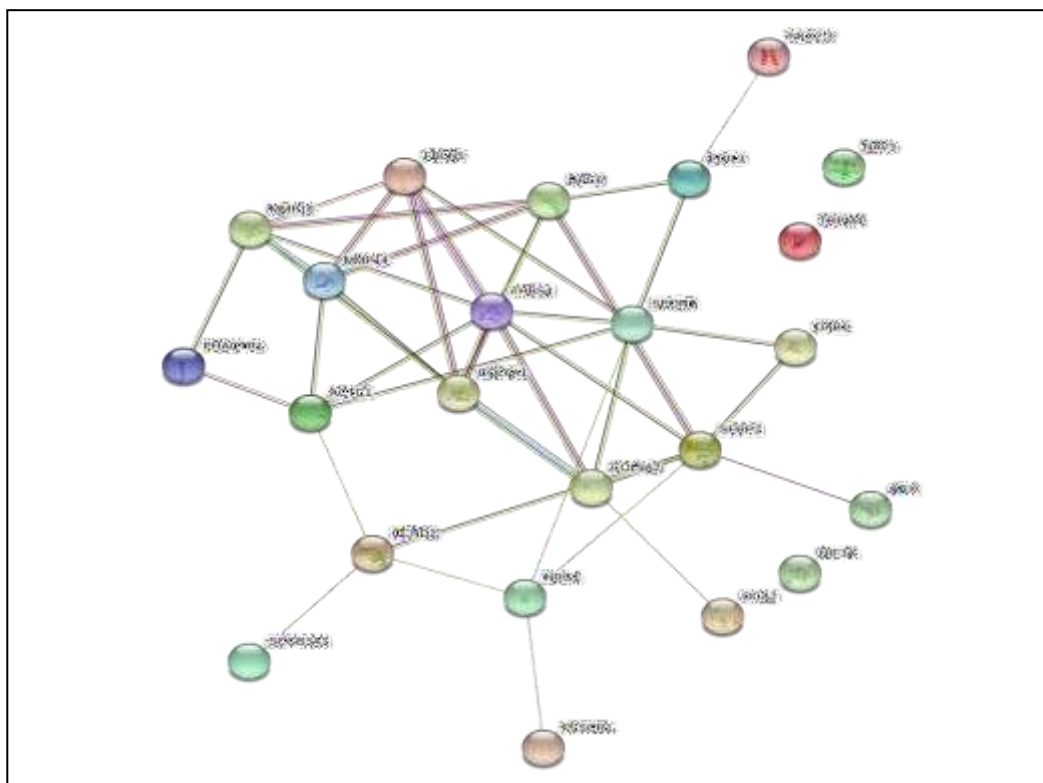
**Figure 14.** KEGG pathway analysis of DEGs and DMGs. Downregulated and hypermethylated genes overlapping. Bars sorted by P-value ranking. KEGG, kyoto encyclopedia of genes and genome. DEGs, differentially expressed genes.





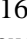


**Figure 15.** KEGG pathway analysis of DEGs. Downregulated and hypomethylated overlapping. Bars sorted by P-value ranking. KEGG, kyoto encyclopedia of genes and genome. DEGs, differentially expressed genes.

**Table 7.** Gene Ontology Enrichment of Biological Processes Terms for DEGs and DMGs.

GO Term	Associated Genes/proteins Found
Regulation of cell population proliferation	ARX, NKX2-3, SCGB3A1, CCND2, TRPM4, NRG1, SFRP2
Cell-matrix organization	FBLN5
Extracellular matrix organization	COL9A2, COL6A1, MMP14, FBLN5, MMP16
Positive regulation of cell division	THBS4
Cell adhesion	SPON1, EDIL3, CCND2, COL6A1, NRG1, DAB1
Regulation of cell growth	SCGB3A1, SFRP2, NRG1, MMP14
Cell migration	GPC6, SFRP2, NAV3, MMP14
Apoptotic process	HIF3A, SFRP2, PLSCR1, CCND2, ACTC1
Regulation of cell motility	NRG1, PHACTR1, MMP14
Cell cycle	OCA2



**Figure 16.** PPI Network of DEGs and DMGs. Gene Ontology Enrichment of Biological Processes. Colored Nodes: Query Proteins and First Shell of Interactors. Line Color Indicates the Type of Interaction Evidence.  Experimentally Determined.  Text Mining.  Co-expression.  From Curated Databases.  Protein Homology.

## Discussion

Cancer is one of the main causes of death worldwide (Siegel, Miller, and Jemal 2016). In Western males, PCa is the most frequently identified cancer and the second leading cause of cancer death. The progression of which may be a consequence of defects in apoptotic machinery (Wen et al. 2014). Thus, the agents who can modulate apoptosis in human PCa cells may be valuable in the therapy of PCa. Phytochemicals are playing an important role currently to treat various diseases and have been proved to significantly treat cancer, without any side effects (Cragg, Newman, and Snader 1997). Plants rich in phytoestrogens were used in nutrition. In recent years, flavonoids have concerned many scientists, due to its putative health-promoting activities possibly resulting from its antioxidant effects. Still, its overall biological impact remains controversial, generally because of incomplete information about its bioavailability, endogenous dynamics, and the relative contribution of different types of conjugates in humans and animals.



As we know, the extracellular matrix (ECM) consists of a complex mixture of structural and functional macromolecules and serves an important role in tissue and organ morphogenesis and the maintenance of cell and tissue structure and function. Specific interactions between cells and the ECM are mediated by transmembrane molecules, mainly integrins and other cell-surface-associated components. These interactions lead to direct or indirect control of cellular activities such as adhesion, migration, differentiation, proliferation, and apoptosis (Stewart, Cooper, and Sikes 2004).

At the cell-extracellular matrix contact points, specialized structures are formed and termed focal adhesions, where bundles of actin filaments are anchored to transmembrane receptors of the integrin family through a multi-molecular complex of junctional plaque proteins. Cell-matrix adhesions play essential roles in important BP including cell motility, cell proliferation, cell differentiation, regulation of gene expression and cell survival (Buskermolen, Kurniawan, and Bouten 2018) Phosphatidylinositol 3-kinase (PI3K)/protein kinase B (AKT) is one of the signaling pathways proven to serve an important role in regulating cell proliferation, the cell cycle, and apoptosis (Shi et al. 2019).

According to the bioinformatics analysis. DEGs and DMGs were mainly associated with ECM-receptor interaction, focal adhesion, PI3K-Akt pathway, ferroptosis, fatty acid synthesis, protein adhesion, longevity regulating pathways, parathyroid hormone synthesis, secretion, and action. Along with the regulation of cell growth, migration, motility, and several different pathways (Table 7). Thrombospondin 4 (THBS4) is an adhesive glycoprotein that mediates cell-to-cell and cell-to-matrix interactions and is involved in various processes including cellular proliferation, migration, adhesion, and attachment. Several studies have investigated its involvement in cancer cell migration and invasion.

Liu et al. evaluated the effects of forced THBS4 knockdown in the two PCa cell lines, DU145 and PC-3 using cell migration and invasion assays. As a result, knockdown of THBS4 significantly reduced the migratory and invasive abilities of the PCa cells in vitro. (Liu et al. 2016). By the same token, McCart Reed et al. also studied the effect of THBS4 knockdown on migration and invasion of hepatocellular carcinoma (HCC). McCart Reed et al. identified that THBS4 is significantly overexpressed in HCC samples and is correlated with prognosis by analyzing the Cancer Genome Atlas Network (TCGA) dataset. The study revealed that knocking down THBS4 inhibits migration and invasion of HCC cells (McCart Reed et al. 2013). Therefore, silencing or targeting THBS4 may provide a promising therapeutic strategy for inhibition and treatment of PCa.

Secretoglobin Family 3A Member 1 (SCGB3A1) a secreted cytokine-like protein that participates in cell growth inhibition in vitro. In this study, SCGB3A1 was found to be downregulated and hypermethylated. Some evidence reported that SCGB3A1 found to be hypermethylated in PCa. According to The Cancer Genome Atlas (TCGA) data analysis, Geybels et al. informed that the top-ranked DMGs included three genes that were associated with both hypermethylation and downregulation namely, SCGB3A1, HIF3A, and AOX1. (Geybels et al. 2015). Whereas Gurioli et al. assessed the methylation status of 40 tumor suppressor genes in healthy prostatic and PCa tissues. The study showed that five genes were

found to be highly methylated in PCa: These genes are GSTP1, RARB, RASSF1, SCGB3A1, and CCND2. The authors emphasized that the hypermethylation of these genes was highly tumor-specific in PCa tissue (Gurioli et al. 2016).

To relate this finding with previous results (Sonbol and Hosawi 2022) we supposed that our extract might affect these genes ARX, NKX2-3, SCGB3A1, CCND2, TRPM4, NRG1, SFRP2, THBS4, MMP14, HIF3A, PLSCR1, OCA2, and ACTC1 that take part in the regulation of cell proliferation, division, growth, cell cycle, and apoptotic process this is likely to have a role in cell death in MTT assay. However, in the scratch assay outcome, the width of the scratch area seems to be lessened as the dose and time increase in untreated cells and treated cells with 0.5 and 5 µg/ml. But, in wells with higher concentrations of *C. cartilaginea* fruit extract 10-20 µg/ml the width of the scratch area widely opened and cells appear to die rather than moving across the scratch, we assumed that this could be due to the effect of the extract on FBLN5, COL9A2, COL6A1, MMP14, MMP16, SPON1, EDIL3, CCND2, NRG1, DAB1, GPC6, SFRP2, NAV3, and PHACTR1 genes that participate in the organization of cell-matrix, extracellular matrix. Also participate in regulating cell adhesion, migration, and motility. Once again, we could refer this observation to the effect of the extract on ARX, NKX2-3, SCGB3A1, CCND2, TRPM4, NRG1, SFRP2, THBS4, MMP14, HIF3A, PLSCR1, OCA2, and ACTC1 genes.

At last, the present study conducted a comprehensive bioinformatics analysis of DEGs and DMGs which may be involved in PCa progression. Our preliminary results highlighted the genes that may provide novel insights into targets that can be used for the future investigation of molecular mechanisms underlying PCa. However, the specific functions of the identified genes in PCa should be confirmed by further molecular biological experiments. Briefly, the in vitro scratch assay is an easy, low-cost and well-developed method to measure cell migration in vitro. The in vitro scratch assay is particularly suitable for studies on the effects of cell-matrix and cell-cell interactions on cell migration, mimic cell migration during wound healing in vivo (Liang, Park, and Guan 2007). Our findings concluded that the *C. cartilaginea* fruit extract may have medicinal properties against PCa 22RV1 cell line affecting cell migratory capacity as the total scratch area widely opened and numbers of dead cells increased nearby ~ 70%. These results increase our knowledge of the wound-healing effects of the investigated plant. Nevertheless, further studies are necessary to find out the effective compounds and secondary metabolites responsible for the observed effects.

## Reference:

1. Globocan (2020). Global Cancer Statistics. Switzerland: Globocan.
2. Panigrahi, G., Praharaj, P., Kittaka, H., Mridha, A., Black, O., Singh, R., Et Al. (2019) Exosome Proteomic Analyses Identify Inflammatory Phenotype And Novel Biomarkers In African American Prostate Cancer Patients, *Cancer Med.*, Vol. 8 (3): 1110-1123. Doi:10.1002/Cam4.1885
3. Osman, Z., And Ibrahim, Z. (2018) Prostate Cancer In The Arab Population. An Overview, *Saudi Med. J.*, Vol. 39 (5): 453-458. Doi:10.15537/Smj.2018.5.21986

4. Belkahl, S., Nahvi, I., Biswas, S., Nahvi, I. And Ben Amor, N. (2022) Advances And Development Of Prostate Cancer, Treatment, And Strategies: A Systemic Review, *Front. Cell Dev. Biol.*, Vol., 10: 991330. Doi: 10.3389/Fcell.2022.991330
5. Vogelstein, B., Papadopoulos, N., Velculescu, V., Zhou, S., Diaz, L. And Kinzler, K. (2013) Cancer Genome Landscapes, *Science.*, Vol. 339: 1546-1558. Doi: 10.1126/Science.1235122.
6. Clough, E. And Barrett, T. (2016) The Gene Expression Omnibus Database, *Methods In Molecular Biology.*, Vol. 1418(5235): 93-110. Doi: 10.1007/978-1-4939-3578-9\_5.
7. Bilir, B., Sharma, V., Lee, J., Hammarstrom, B., Svindland, A., Kucuk, O. And Moreno, S. (2017) Effects Of Genistein Supplementation On Genome-Wide Dna Methylation And Gene Expression In Patients With Localized Prostate Cancer, *International Journal Of Oncology.*, Vol. 51: 223-234.
8. Meller, S., Meyer, A., Bethan, B., Dietrich, D., Maldonado, G., Lein, M., Et Al. (2016) Integration Of Tissue Metabolomics, Transcriptomics And Immunohistochemistry Reveals Erg- And Gleason Score-Specific Metabolomic Alterations In Prostate Cancer, *Oncotarget.*, Vol. 7: 1421-1438.
9. Oliveros, J.C. (2007-2015) Venny. An Interactive Tool For Comparing Lists With Venn's Diagrams, Access Date, November 25, 2019, From: <https://Bioinfogp.Cnb.Csic.Es/Tools/Venny/Index.Html>
10. Wu, C., Jin, X., Tsueng, G., Afrasiabi, C. And Su, A. (2016) Biogps: Building Your Own Mash-Up Of Gene Annotations And Expression Profiles, *Nucl. Acids Res.*, Vol. 44: D313-D316.
11. Stelzl, U., Worm, U., Lalowski, M., Haenig, C., Brembeck, F., Goehler, H., Et Al. (2005) A Human Protein-Protein Interaction Network: A Resource For Annotating The Proteome, *Cell.*, Vol. 122(6): 957-968. Doi: 10.1016/J.Cell.2005.08.029.
12. Von Mering, C., Huynen, M., Jaeggi, D., Schmidt, S., Bork, P., Sne, L B. (2003) String: A Database Of Predicted Functional Associations Between Proteins, *Nucleic Acids Research.*, Vol. 31(1): 258-261. Doi: 10.1093/Nar/Gkg034
13. Szklarczyk, D., Franceschini, A., Wyder, S., Forslund, K., Heller, D., Huerta-Cepas, J., Et Al. (2015) String V10: Protein-Protein Interaction Networks, Integrated Over The Tree Of Life, *Nucleic Acids Res.*, Vol. 43:D447-D452.
14. Franceschini, A., Szklarczyk, D., Frankild, S., Kuhn, M., Simonovic, M., Roth, A., Et Al. (2013) String V9. 1: Protein-Protein Interaction Networks, With Increased Coverage And Integration, *Nucleic Acids Res.*, Vol. 41: D808-D815.
15. Kuleshov, M., Jones, M., Rouillard, A., Fernandez, N., Duan, Q., Wang, Z., Et Al. (2016) Enrichr: A Comprehensive Gene Set Enrichment Analysis Web Server 2016 Update, *Nucleic Acids Research.*, Vol. 44(W1): W90-W97.
16. Chen, E., Tan, C., Kou, Y., Duan, Q., Wang, Z., Meirelles, G., Clark, N. And Ma'ayan, A. (2013) Enrichr: Interactive And Collaborative Html5 Gene List Enrichment Analysis Tool, *Bmc Bioinformatics.*, Vol. 128: 14.

17. Kanehisa, M. And Goto, S. (2000) Kegg: Kyoto Encyclopedia Of Genes And Genomes, Nucleic Acids Res., Vol. 28: 27-30.
18. The Uniprot Consortium., (2019) Uniprot: A Worldwide Hub Of Protein Knowledge,
19. Theodorescu, D., Laderoute, K., Calaoagan, J. And Guilding, K. (1998) Inhibition Of Human Bladder Cancer Cell Motility By Genistein Is Dependent On Epidermal Growth Factor Receptor But Not P21ras Gene Expression, Int J Cancer., Vol. 78: 775-782.
20. Siegel, R., Miller, K. And Jemal, A. (2016) Cancer Statistics, 2016, Ca Cancer J Clin., Vol. 66: 7-30.
21. Wen, J., Li, R., Wen, X., Et Al. (2014) Dysregulation Of Cell Cycle Related Genes And Micrnas Distinguish The Low- From High-Risk Of Prostate Cancer, Diagn Pathol., Vol. 9:156.
22. Cragg, G., Newman, D. And Snader, K. (1997) Natural Products In Drug Discovery And Development, J Nat Prod., Vol. 60:52-60.
23. Stewart, D., Cooper, C. And Sikes, R. (2004) Changes In Extracellular Matrix (Ecm) And Ecm-Associated Proteins In The Metastatic Progression Of Prostate Cancer, Reprod Biol Endocrinol., Vol. 2: 2.
24. Buskermolen, A., Kurniawan, N. And Bouten, C. (2018) An Automated Quantitative Analysis Of Cell, Nucleus And Focal Adhesion Morphology, Plos One., Vol. 13: E0195201.
25. Shi, X., Wang, J., Lei, Y., Cong, C., Tan, D. And Zhou, X. (2019) Research Progress On The Pi3k/Akt Signaling Pathway In Gynecological Cancer (Review), Molecular Medicine Reports., Vol. 19: 4529- 4535.
26. Liu, J., Cheng, G., Yang, H., Deng, X., Qin, C., Hua, L. And Yin, C. (2016) Reciprocal Regulation Of Long Noncoding Rnas Thbs4-003 And Thbs4 Control Migration And Invasion In Prostate Cancer Cell Lines, Mol Med Rep., Vol. 14: 1451-1458.
27. McCart Reed, A., Song, S., Kutasovic, J., Reid, L., Valle, J., Vargas, A., Smart, C. And Simpson, P. (2013) Thrombospondin-4 Expression Is Activated During The Stromal Response To Invasive Breast Cancer, Virchows Arch., Vol. 463: 535-545.
28. Geybels, M., Zhao, S., Wong, C., Bibikova, M., Klotzle, B., Wu, M., Ostrander, E., Fan, J., Feng, Z. And Stanford, J. (2015) Epigenomic Profiling Of Dna Methylation In Paired Prostate Cancer Versus Adjacent Benign Tissue, Prostate., Vol. 75: 1941-1950.
29. Gurioli, G., Salvi, S., Martignano, F., Foca, F., Gunelli, R., Costantini, M., Cicchetti, G., Giorgi, U., Sbarba, P., Calistri, D. And Casadio, V. (2016) Methylation Pattern Analysis In Prostate Cancer Tissue: Identification Of Biomarkers Using An Ms-Mlpa Approach, J Transl Med., Vol. 14: 249.
30. Sonbol, H., And Hosawi, M. (2022). Flavonoids Of Capparis Cartilaginea Fruit Extract Effect On Wound Healing In Human Prostate Cancer Cell Line, Pharmacophore., Vol. 13(5): 127-137.

31. Liang, C., Park, A. And Guan, J. (2007) In Vitro Scratch Assay: A Convenient And Inexpensive Method For Analysis Of Cell Migration In Vitro, Nat Protoc., Vol. 2: 329-333.